⌘ *Author's Choice*

THE JOURNAL OF BIOLOGICAL CHEMISTRY VOL. 287, NO. 14, pp. 11516–11525, March 30, 2012

Rapid Aquaporin Translocation Regulates Cellular Water Flow

*MECHANISM OF HYPOTONICITY-INDUCED SUBCELLULAR LOCALIZATION OF AQUAPORIN 1 WATER CHANNEL**

Received for publication, December 20, 2011, and in revised form, January 23, 2012 Published, JBC Papers in Press, February 9, 2012, DOI 10.1074/jbc.M111.329219

Matthew T. Conner[‡12], Alex C. Conner[§1], Charlotte E. Bland[‡], Luke H. J. Taylor[§], James E. P. Brown[‡], H. Rheinallt Parri[‡], and Roslyn M. Bill[‡3]

From the [‡]School of Life & Health Sciences and Aston Research Centre for Healthy Ageing, Aston University, Aston Triangle, Birmingham B4 7ET, United Kingdom, and the [§]Warwick Medical School, University of Warwick, Coventry CV4 7AL, United Kingdom

Background: Aquaporin channels ensure appropriate membrane permeability to water in all cells.
Results: Following a hypotonic stimulus, subcellular localization of aquaporin 1 occurs via a mechanism dependent on transient receptor potential channels, extracellular calcium influx, calmodulin, and the phosphorylation of two threonines (157 and 239) of aquaporin 1.
Conclusion: Rapid translocation of aquaporin 1 regulates membrane water permeability.
Significance: This mechanism may serve as a prototype for the rapid regulation of aquaporin function.

The control of cellular water flow is mediated by the aquaporin (AQP) family of membrane proteins. The structural features of the family and the mechanism of selective water passage through the AQP pore are established, but there remains a gap in our knowledge of how water transport is regulated. Two broad possibilities exist. One is controlling the passage of water through the AQP pore, but this only has been observed as a phenomenon in some plant and microbial AQPs. An alternative is controlling the number of AQPs in the cell membrane. Here, we describe a novel pathway in mammalian cells whereby a hypotonic stimulus directly induces intracellular calcium elevations through transient receptor potential channels, which trigger AQP1 translocation. This translocation, which has a direct role in cell volume regulation, occurs within 30 s and is dependent on calmodulin activation and phosphorylation of AQP1 at two threonine residues by protein kinase C. This direct mechanism provides a rationale for the changes in water transport that are required in response to constantly changing local cellular water availability. Moreover, because calcium is a pluripotent and ubiquitous second messenger in biological systems, the discovery of its role in the regulation of AQP translocation has ramifications for diverse physiological and pathophysiological processes, as well as providing an explanation for the rapid regulation of water flow that is necessary for cell homeostasis.

The flow of water across cell membranes is fundamental to the physiology of all organisms. It is now clear that osmosis is not sufficient for this purpose; rather aquaporin (AQP)[4] channels are required to ensure appropriate membrane permeability to water molecules (1, 2). Over the past two decades, the molecular basis of selective water passage through the AQP pore (3, 4), as well as the structural biology of the family (5), have been established. However, there is a gap in our current understanding of how AQPs regulate the flow of water in and out of cells to meet the constant and rapid changes in local water availability that challenge them.

Membrane permeability to water is a function of the properties of the AQP pore as well as the abundance of AQP molecules in the cell membrane. The AQP pore is acknowledged widely to be constitutively open and highly specific. Some AQPs are permeable only to water, whereas others (*e.g.* the aquaglyceroporins) are permeable to both water and small non-ionic molecules such as glycerol, urea, and ammonia (3, 4, 6). Regulation via gating mechanisms, which allow open and closed states, has been reported for some plant and microbial AQPs (7). However, this is not a widely accepted regulatory mechanism for mammalian AQPs (8).

Regulation of AQP abundance, the number of pores per unit plasma membrane, is possible *via* several mechanisms. Direct regulation by AQP gene expression and/or AQP protein degradation can be achieved over a time scale from hours to days (9, 10). Indirect, receptor-mediated mechanisms (11, 12) also have been described that account for more rapid regulation of AQP abundance on a time scale of minutes (13, 14). The best studied example of this is the regulation of AQP2 translocation in human kidney cells, which is dependent on vasopressin-medi-

* This work was supported by European Commission Framework Programme 7 Grant 201924 EDICT (to R. M. B.).
⌘ *Author's Choice*—Final version full access.
[1] Both authors contributed equally to this work.
[2] Present address: Biomedical Research Centre, Sheffield Hallam University, Howard Street, Sheffield S1 1WB, United Kingdom.
[3] To whom correspondence should be addressed: School of Life & Health Sciences and Aston Research Centre for Healthy Ageing, Aston University, Aston Triangle, Birmingham, B4 7ET UK. Tel.: 0121-204-4274; E-mail: r.m.bill@aston.ac.uk.

[4] The abbreviations used are: AQP, aquaporin; CPA, cyclopiazonic acid; Myr, myristoylated; TRPC1, transient receptor potential channel 1; CAM, calmodulin; PMA, phorbol 12-myristate 13-acetate; RME, relative membrane expression.

ated activation of protein kinase A by the G protein-coupled receptor, vasopressin V_2 receptor (15). Of the 13 known AQPs in the human body, AQP1 (16), AQP3 (17), and AQP5 (18) also have been shown to undergo translocation to the plasma membrane in response to hormonal activation of specific G protein-coupled receptors.

Neither gene expression nor indirect, receptor-mediated translocation can explain the direct regulation of AQPs that may be necessary to respond to the rapidly changing extracellular environment on a time scale of seconds. We recently demonstrated that increased translocation of AQP1 is triggered on this rapid timescale by hypotonic stimulus in a specific protein kinase C (PKC)- and microtubule-dependent manner (19). Furthermore, returning the extracellular environment to its original tonicity reversed this dynamic subcellular localization. In contrast, a hypotonic stimulus had little effect on AQP2 localization in the absence of the vasopressin V_2 receptor required for AQP2 translocation (19).

The change in cell volume that results from the transport of water across biological membranes is thought to be dependent on PKC and calcium, as well as the presence of transient receptor potential (TRP) channels and AQPs (20–22). The data presented here provide evidence of a mechanistic link between these elements. In this study, we combined laser scanning confocal microscopy of chimeras of AQP1 with green fluorescent protein (AQP1-GFP), calcium imaging, and mutagenesis to determine that AQP1 translocation underpins the regulation of cellular water flow, as measured by changes in cell volume. Our data show that manipulating rapid AQP1 translocation, which can be observed in primary astrocytes as well as model cell lines, modulates changes in cell volume and that this rapid subcellular localization of AQP1 requires extracellular calcium influx, TRP channels, calmodulin, and specific phosphorylation at two known PKC sites, Thr-157 and Thr-239. We therefore suggest that the regulation of AQPs provides the rapid homeostatic control required by cells in a constantly changing osmotic environment.

EXPERIMENTAL PROCEDURES

Materials—Cell-permeable inhibitors were purchased as follows: phorbol 12-myristate 13-acetate (PMA; $ED_{50} \sim 1$ nM (23)), 1-oleoyl-2-acetyl-*sn*-glycerol (ED_{50} in μM range but more specific than PMA (24, 25)), caffeine ($K_d \sim 10$ nM (26)), and W7 calmodulin antagonist (*N*-(6-aminohexyl)–5-chloronaphthalene-1-sulfonamide; $K_d \sim 1$ μM (27, 28)) from Sigma; TRPC1 antagonist SKF96365 (10 mM concentrations are utilized typically to assay TRPC function (29)) from Ascent Scientific, Ltd. (Bristol, UK); Myr-PKC 19–27 and hypericin ($K_d \sim 100$ nM (30)) from Fisher Scientific (Loughborough, UK); Myr-PKA 14–22 from Merck Chemicals (Nottingham, UK); and CPA (cyclopiazonic acid; inhibits sarco/endoplasmic reticulum Ca^{2+}-ATPase with nanomolar affinity (31)) from Tocris Bioscience (Bristol, UK). Fluorodish™ dishes were from WPI, Ltd. (Stevenage, UK). Polyclonal rabbit anti-AQP1 was from Alamone (Jerusalem, Israel), secondary goat anti-rabbit IgG-FITC was from Santa Cruz Biotechnology (Santa Cruz, CA), and monoclonal anti-glial fibrillary acidic protein antibody was from Millipore. Gateway vectors and enzymes were from Invitrogen. Unless otherwise specified, all other chemicals were from Sigma or Fisher. Cell culture reagents were from Invitrogen or Sigma. In each experiment, all inhibitors and activators were analyzed using wild-type AQP1-GFP as a control.

Expression Constructs and Mutagenesis—AQPs were fused with carboxyl-terminal GFP using the Invitrogen Gateway™ cloning system according to the manufacturer's instructions. Sequence-verified AQP cDNAs were a kind gift of Dr. Kristina Hedfalk (Göteborg University). For directional cloning of blunt-ended PCR products into an entry vector using the Gateway™ system, four bases (GGGG) were added to the 5′-end of the forward primer followed by the 25-bp *att*B1 attachment sequence (underlined). This was followed by five bases (boldface type) to introduce a Kozak sequence upstream and to keep the sequence in frame with the AQP coding sequence. Finally, 18–25 bp of the AQP sequence were added to create the amino-terminal forward primers, 5′-GGGG ACA AGT TTG TAC AAA AAA GCA GGC T**CC ACC** ATG-AQP(18–25 bp)-3′. For the reverse primer, four bases (GGGG) were added to the 5′-end followed by the 25-bp *att*B2 attachment sequence (underlined), and then one base (boldface type) was added to keep the sequence in frame with the AQP coding sequence. Finally, 18–25 bp of the AQP sequence without the stop codon were added to create the carboxyl-terminal forward primers 5′-GGG GAC CAC TTT GTA CAA GAA AGC TGG GT**C**–AQP(18–25 bp)-3′. DNA polymerase from *Thermococcus kodakaraensis* (KOD) polymerase was used in PCR amplification of the AQP cDNA. Samples were heated to 94 °C for 2 min, followed by 30 cycles of 94 °C for 30 s, 55 °C for 30 s, and 68 °C for 3 min, and then 68 °C for 7 min. Purified PCR products were subcloned into the pDONR221™ entry vector (Invitrogen) using the *att*B1 and *att*B2 sites in a reaction with Gateway™ BP Clonase™ enzyme mix (Invitrogen). pDONR221™ vectors containing the required sequences were recombined with the pcDNA-DEST47 Gateway™ vector using the *att*L and *att*R reaction with Gateway™ LR Clonase™ enzyme mix (Invitrogen). This created expression vectors with the cycle 3 mutant of the GFP gene at the carboxyl terminus of the AQP gene of interest, which were expressed subsequently as fusion proteins. All mutant constructs were amplified using the well established, modified QuikChange procedure (Stratagene), as described previously (32). All plasmids were handled and purified using standard molecular biological procedures.

Cell Culture and Transfection—HEK 293 cells were cultured routinely in DMEM supplemented with 10% (v/v) fetal bovine serum in humidified 5% (v/v) CO_2 in air at 37 °C. Cells were seeded into 30-mm Fluorodish™ dishes and transfected after 24 h at 50% confluency using the Transfast (Promega) transfection protocol with 3 μg of DNA/dish. Cortices were dissected from neonatal 2–5-day-old Wistar rats and placed in cold HEPES-buffered saline. Following mechanical digestion in modified glial medium (DMEM/F12 culture medium with 10% fetal bovine serum, 1% glutamine, and 10 μg/ml gentamicin), the tissue was digested chemically in 1× trypsin and DNase for 25 min at 37 °C. The tissue was then washed twice with glial medium and dissociated into a cell suspension by trituration three times sequentially through a 5-ml pipette followed by a fire-polished Pasteur pipette. Suspended cells were diluted in

10 ml of glial medium, and passed through a 40 μM strainer. Following centrifugation (500 $\times$ *g* for 5 min), the supernatant was removed, and the pellet was suspended in 10 ml of glial medium. Cells were seeded at 2×10^6 cells/T75 cm^2 flask in 15 ml of glial medium and incubated at 37 °C in 5% CO_2, changing the medium every 2 days until confluency was achieved (~6–7 days). Astrocytes were purified by shaking at 350 rpm for 6 h at 37 °C to separate oligodendrocytes from astrocytes; the glial medium and oligodendrocytes were replaced with fresh medium and shaken for 18 h and then again for a further 24 h changing the medium every 6 h. Cells were reseeded at 3×10^5 cells/T75 cm^2 flask. Identification of primary astrocytes was confirmed by immunocytochemistry.

Primary Astrocyte Immunocytochemistry—Endogenous AQP1 protein was visualized in isolated rat primary astrocytes. Cells grown on coverslips and exposed to glial medium or diluted glial medium were fixed by perfusing (optimized to ensure tonicity changes did not affect expression profile) with 4% (v/v) paraformaldehyde in phosphate-buffered saline for 15 min at room temperature, washed twice with phosphate-buffered saline, and permeabilized using a blocking solution containing 0.25% (v/v) Triton X-100, 1% (v/v) goat serum and 1% (w/v) bovine serum albumin in phosphate-buffered saline. Successive incubations with primary and secondary antibodies were carried out for 16 h at 4 °C and 1 h at room temperature, respectively. Primary antibodies (1:500) were detected by species-specific FITC-conjugated secondary antibodies (1:1,000). Cells were washed in phosphate-buffered saline, and coverslips were mounted with Vectorshield (Vector Laboratories). The cells were visualized, and confocal images were acquired using confocal laser scanning microscopy as described below. Because perfused, fixed primary cells were used, the same live cell could not be compared under differing conditions; rather, cells from the same subcultured population were compared on different cover slips.

Confocal Microscopy—AQP-GFP fusion proteins were visualized in live cells enclosed in a full environmental chamber by confocal laser scanning microscopy. Confocal images were acquired with a Leica SP5 laser scanning microscope and a Zeiss Axiovert 200 m inverted microscope with a 63× (1.4 numerical aperture) oil immersion objective for immunocytochemical analysis or a Zeiss Axiovert 200 m upright microscope with a 20× (1.0 numerical aperture) water dipping objective for live cell analysis. The nucleus and the plasma membrane were stained with DAPI and 5 μg/ml FM4-64 (Molecular Probes), respectively. Images were acquired using an argon laser (excitation, 488 nm; emission, band pass, 505–530 nm) for GFP, UV excitation and a band pass 385–470 nm emission filter for DAPI, and a He-Ne laser (excitation, 543 nm; emission filter, long pass, 650 nm) for FM4-64. 48 h post-transfection, cells in Fluorodishes™ were incubated with or without 50 μM Myr-PKC 19–27, 50 μM Myr-PKA 14–22, 50 μM hypericin, 10 μM 1-oleoyl-2-acetyl-*sn*-glycerol, 5 μM PMA, 10 mM caffeine, 10 μM CPA (30 min), 10 mM TRPC1 antagonist SKF96365 or 100 μM W7 for 1 h at 37 °C and 5% CO_2. For inhibitor and activator experiments, the concentrations used were derived from the literature and were a minimum of 10 $\times$ K_d (where known) to ensure 90% theoretical fractional occupancy of the target protein. Where no effect was seen, the dose was increased: for example, 1,000 $\times$ K_d achieves 99.9% fractional occupancy. The volume of inhibitor (in water) added to the cells was <1% (v/v) to ensure a minimum effect on osmolality. Cells were visualized in control medium (DMEM) that has an inorganic salt concentration of 120 mM, a glucose concentration of 25 mM, and an osmolality in the range 322–374 mosM/kg H_2O. Hypotonic medium has an osmolality in the range 107–125 mosM/kg H_2O through dilution of DMEM by a factor of 3 with water. Protein localization was measured using a line profile (pixel density) traced on each transfected cell. Localization data are representative of three to five cells from at least three independent experiments. Line expression profiles were generated and analyzed with the program ImageJ (http://rsb.info.nih.gov/ij/) and are indicated in *yellow* and displayed below each confocal image.

Determination of Subcellular Localization—A minimum of five line profiles were measured and distributed at regular intervals covering the plasma membrane and the cytosol but avoiding the nucleus of a minimum of three cells from at least three independent experiments. The fluorescence intensity over this distance was measured, and the difference between the peak and the plateau of fluorescence was divided by the maximum fluorescence along the line scan to calculate the percentage of fluorescence at the membrane. This was termed the relative membrane expression (RME) (19). Identification of the plasma membrane was achieved by staining with FM4-64 and overlaying the GFP images. Nuclei were identified though DAPI staining. The overlay of the GFP image either with the bright-field image or the red fluorescence emitted by FM4-64 clearly indicated integration of GFP-tagged AQP1 at the plasma membrane as well as in the cytoplasm of HEK293 cells.

Calcium Imaging—Calcium analysis was performed as described previously (33). Briefly, transfected cells were loaded with Fluo-4 AM (Invitrogen) by incubating for 40–60 min at 37 °C with 10 μM of the indicator dye and 0.01% pluronic acid. Cells were placed in a recording chamber with a moveable platform (MP MTP-01, Scientifica, Uckfield, UK) fitted to a Nikon FN-1 upright microscope. Whole-field images were acquired routinely every 5 s with a 20× objective lens using a fluorescence imaging system equipped with a Cairn optoscan monochromator (Cairn Research, Faversham, UK) and an Hamamatsu ORCA-ER camera (Digital Pixel, Brighton, UK). Typical exposure to the selected monochromator light wavelength was 50–100 ms every 1–5 s.

Estimation of Cell Volume—10-Hz confocal x-y images of the same cell under both isotonic and hypotonic conditions were converted to binary format using ImageJ software. The comparative z-position was maintained and confirmed by the appropriation of the z-plane with the largest surface area as well as cross-referencing fluorescence intensity from other areas of the selected image (34). The surface area was then calculated using particle analysis software in ImageJ. Each estimate of cell volume was made from at least 10 independent cells from at least three separate experimental determinations.

RESULTS

Endogenous AQP1 Translocation Is Triggered by Hypotonic Stimulus—AQP1 is found in diverse tissues (35), including astrocytes (36). To confirm the physiological relevance of hypotonicity-triggered AQP1 translocation, pri-

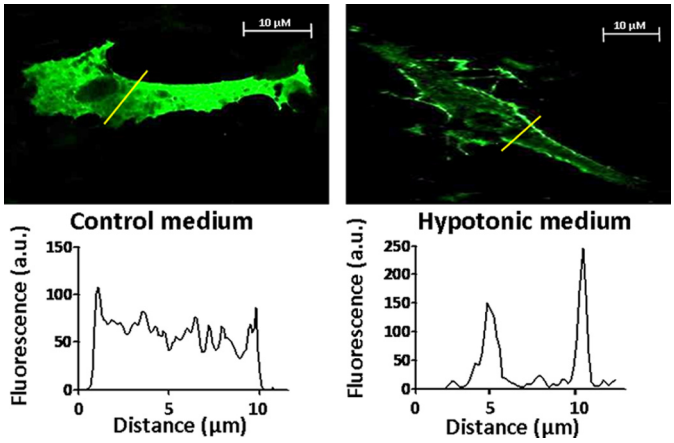

FIGURE 1. **AQP1 subcellular localization in fixed, primary rat astrocytes.** Immunocytochemistry showing expression profiles of endogenous AQP1 in primary rat astrocytes. Cells shown in each representative image are different fixed cells from the same subculture exposed to different osmotic conditions. Fluorescence amplitudes (*a.u.*, arbitrary units) along the line scans (in *yellow* on the image) are displayed graphically *below* each image. RME is calculated from at least five line scan analyses performed in triplicate on a minimum of three independent experiments. Control medium and hypotonic medium are DMEM and F12 at a ratio of 1:1 with osmolalities of 322–374 mosM/kg H_2O and 107–125 mosM/kg H_2O (diluted with water), respectively. All images and analyses shown are a single representation contributing to the mean value quoted in the text and in Table 1.

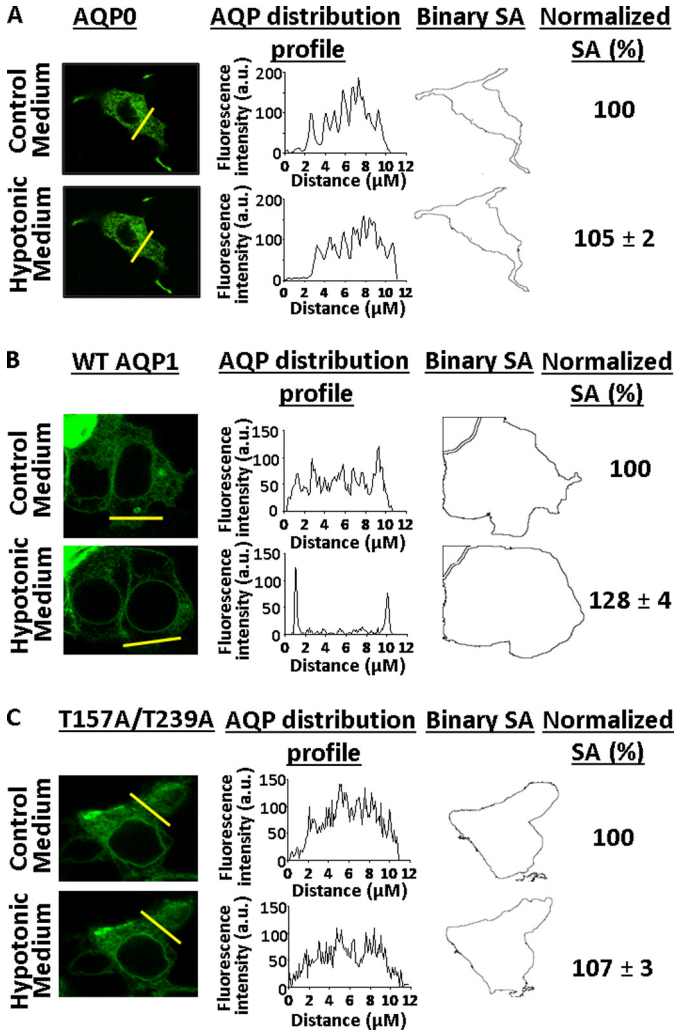

FIGURE 2. **Regulation of hypotonicity-induced increase in cell volume by AQP1 translocation in HEK293 cell.** Representative images showing x-y surface area (*SA*) estimation of cell volume. The binary image and surface area are calculated from the z-stack plane at the maximum area. All measurements were taken at 48 h post-transfection. *A*, HEK293 cells transfected with wild-type AQP0-GFP. *B*, HEK293 cells transfected with wild-type AQP1-GFP. *C*, HEK293 cells transfected with the T157A/T239A translocation-deficient mutant of AQP1-GFP. Control medium and hypotonic medium are DMEM with osmolalities of 322–374 mosM/kg H_2O and 107–125 mosM/kg H_2O (diluted with water), respectively. Distribution profiles along the line scans (in *yellow* on the image) are displayed graphically by each image indicating AQP distribution in control and hypotonic medium (*a.u.* is arbitrary units). All images and analyses shown are a single representation contributing to the mean value quoted in the text and in Table 1.

mary astrocytes from rat cortex were stimulated hypotonically, perfused with formaldehyde, and examined using confocal microscopy. GFAP (glial fibrillary acidic protein) staining confirmed the astrocytic phenotype of the cells. Immunostaining with an anti-AQP1 antibody suggested increased plasma membrane localization of endogenous AQP1: the RME significantly increased from 30 ± 10% to 62 ± 9%, $p < 0.01$, following hypotonic stimulus (Fig. 1). Interestingly, increased nuclear membrane staining was also apparent in the primary astrocytes (Fig. 1). These results are in agreement with our previous studies using heterologous GFP-tagged AQP1 in HEK293 cells (19). HEK293 cells transfected with heterologous, GFP-tagged AQP1 were therefore used as a model for AQP translocation, allowing live cell imaging of individual, treated cells (compared with the fixed astrocytes), and analysis of AQP mutants. This model was used for all subsequent experiments.

Cell Volume Increases with AQP1 Translocation—To establish that functional AQP1 was inserted into the plasma membrane, a cell-swelling assay was performed as it is established that aquaporins function by allowing water movements across membranes (1, 2). Following hypotonic exposure, cell volume was estimated using x-y surface area measurement at the z-stack plane of maximal area (34). HEK293 cells transfected with AQP0, which does not show increased localization at the plasma membrane (19) had an increase in surface area of 5 ± 2% (compared with cells in DMEM) after a 30-s hypotonic exposure ($p < 0.01$; Fig. 2*A*) compared with 28 ± 4% for cells transfected with AQP1-GFP ($p < 0.01$; Fig. 2*B*). This increase was sustained for at least 15 min and was fully reversible on removal of the hypotonic stimulus. These functional experiments correlate aquaporin translocation (as measured by the fluorescence distribution profiles) to functional cell swelling, strongly suggesting that functional AQP1 is inserted into the plasma membrane.

Phosphorylation at Both PKC Sites Is Necessary for AQP1 Translocation—To establish a causal relationship between AQP1 translocation and the estimated increase in cell volume, we searched for mutant forms of AQP1 that would not translocate and therefore should not affect cell volume. We previously showed that the PKC inhibitor, Myr-PKC 19–27, ablates rapid hypotonicity-mediated membrane translocation of AQP1 (19). In peptide mimetic studies, PKC has also been demonstrated to phosphorylate AQP1 at T157 and T239 (37), although no effect on translocation was measured. We therefore mutated the PKC-dependent threonine

TABLE 1

Relative membrane expression and calcium responses of HEK293 cells expressing AQP1 or AQP1 mutants

Experiments were performed in HEK293 cells expressing the proteins indicated and cultured in the specified medium. RME values are the mean ± S.E. of at least five line scan analyses performed in triplicate on a minimum of three independent experiments. The intracellular calcium ($[Ca^{2+}]_i$) responses are the mean ± S.E. of 100 individual cell trace analyses of a minimum of three independent experiments. CaM indicates calmodulin, and OAG indicates 1-oleoyl-2-acetyl-*sn*-glycerol.

Construct/initial medium	RME initial medium	RME following hypotonic stimulus	Hypotonicity-induced translocation of AQP	Hypotonicity-induced $[Ca^{2+}]_i$ response (% of basal $[Ca^{2+}]_i$)
Wild-type AQP1-GFP				
Control medium	19 ± 3%	73 ± 5%	Y	40 ± 7%
CPA	18 ± 4%	71 ± 9%	Y	43 ± 12%
Extracellular calcium-free medium	21 ± 4%	24 ± 4%	N	0 ± 1%
Extracellular calcium-free medium + CPA	23 ± 3%	25 ± 5%	N	1 ± 1%
Myr-PKC 19–27 inhibitor	21 ± 2%	24 ± 3%	N	33 ± 6%
Hypericin PKC inhibitor	22 ± 4%	23 ± 3%	N	
W7 CAM inhibitor	25 ± 4%	28 ± 6%	N	38 ± 7%
SKF96365 TRPC1 antagonist	26 ± 5%	25 ± 6%	N	
PMA PKC activator	20 ± 2%	75 ± 4%	Y	
OAG PKC activator	22 ± 5%	71 ± 7%	Y	
Caffeine	26 ± 4%	72 ± 6%	y	
T157A AQP1-GFP				
Control medium	22 ± 3%	75 ± 2%	Y	34 ± 5%
T239A AQP1-GFP				
Control medium	21 ± 5%	81 ± 9%	Y	32 ± 6%
T157D AQP1-GFP				
Control medium	24 ± 3%	73 ± 6%	Y	35 ± 4%
T239D AQP1-GFP				
Control medium	18 ± 5%	69 ± 9%	Y	37 ± 6%
T157A/T239A AQP1-GFP				
Control medium	21 ± 5%	21 ± 2%	N	46 ± 10%
T157D/T239D AQP1-GFP				
Control medium	23 ± 4%	75 ± 7%	Y	40 ± 7%
Myr-PKC 19–27 inhibitor	24 ± 6%	78 ± 8%	Y	
Hypericin PKC inhibitor	23 ± 5%	72 ± 6%	Y	
W7 calmodulin antagonist	28 ± 5%	22 ± 4%	N	

residues of AQP1, individually, to alanine to remove the putative phosphorylation site, and to aspartate to mimic the charge induced by phosphorylation of threonine. This created the AQP1-GFP mutants, T157A, T239A, T157D, and T239D. Surprisingly, all four single mutants translocated to the plasma membrane in hypotonic medium: the RMEs in control medium were 22 ± 3%, 21 ± 5%, 24 ± 3%, and 18 ± 5%, respectively, and were 75 ± 2%, 81 ± 9%, 73 ± 6%, and 69 ± 9% in hypotonic medium, respectively (Table 1). This indicated that mutation of each putative phosphorylation site affected neither AQP1 translocation nor its constitutive surface localization.

In contrast, double mutation of both putative PKC phosphorylation sites to alanine, creating the mutant T157A/T239A, completely ablated hypotonicity-induced translocation of AQP1-GFP: the RME in control medium was 21 ± 5% and in hypotonic medium was 21 ± 2% (Table 1) even after 15 min of exposure. Double mutation of both putative PKC phosphorylation sites to aspartate created the phosphomimetic mutant T157D/T239D. As expected, T157D/T239D translocated to the plasma membrane following hypotonic exposure (RME in control medium was 23 ± 4% rising to 75 ± 7% in hypotonic medium; Table 1). We concluded that although the double aspartate mutant, T157D/T239D, was not constitutively expressed at the cell surface, it is primed for rapid translocation to the membrane following hypotonic exposure.

AQP1 Translocation Regulates Changes in Cell Volume—Changes in cell volume were estimated for cells transfected with mutant AQP1 constructs. After a 30-s hypotonic exposure, HEK293 cells transfected with the translocation-deficient mutant T157A/T239A had an increase of 7 ± 3% compared with cells in DMEM ($p < 0.01$; Fig. 2*C*). Cell volume was not significantly different from wild-type ($p > 0.05$) for all four single mutants (T157A, T239A, T157D, and T239D) or the T157D/T239D mutant. The difference in hypotonicity-induced volume change between cells transfected with wild-type AQP1-GFP (28 ± 4%; Fig. 2*B*) and those transfected with the translocation-deficient mutant (T157A/T239A) supports an interpretation that AQP1 translocation to the plasma membrane regulates changes in cell volume in response to hypotonic conditions.

Phosphorylation Is Not Sufficient for Hypotonicity-induced AQP1 Translocation—Incubation of cells expressing AQP1-GFP with either the specific PKC inhibitor Myr-PKC 19–27 (19) or hypericin PKC inhibitor, inhibited hypotonicity-induced subcellular localization of wild-type AQP1-GFP (Table 1). We reasoned that if the T157D/T239D mutant was a mimic of a doubly phosphorylated state and hence was primed for localization, these compounds should not inhibit its translocation; indeed, no inhibition of hypotonicity-induced translocation was observed (Table 1). The RME for T157D/T239D in the presence of Myr-PKC 19–27 was 24 ± 6% in control medium rising to 78 ± 8% in hypotonic medium. In the presence of hypericin the RME values of T157D/T239D were 23 ± 5% in control medium and 72 ± 6% in hypotonic medium. Importantly, the PKC activators, PMA and 1-oleoyl-2-acetyl-*sn*-glycerol, did not stimulate wild-type AQP1 translocation in control medium (following incubation with PMA or 1-oleoyl-2-acetyl-*sn*-glycerol, RME

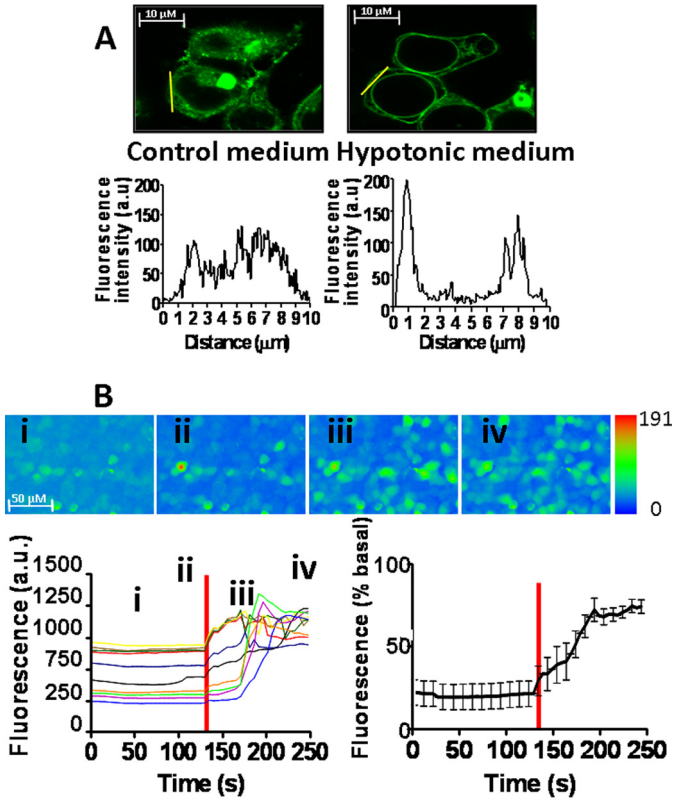

FIGURE 3. **Hypotonicity-induced intracellular Ca^{2+} elevations and AQP1 translocation in HEK293 cells.** *A*, subcellular localization of AQP1-GFP fusion proteins in HEK293 cells before and after hypotonic stimulus. The same living cells are shown in control medium (*left panel*) and in hypotonic medium (*right panel*). All measurements were taken at 48 h post-transfection. Fluorescence amplitudes along the line scans (in *yellow* on the image) are displayed graphically below each image indicating translocation of AQP1-GFP in response to hypotonic stimulus (*a.u.* is arbitrary units). RME is calculated from at least five line scan analyses performed in triplicate on a minimum of three independent experiments. *B*, individual traces of calcium fluorescence *versus* time (*lower left panel*) for 10 randomly selected cells from the images in the *top panels* (scale in arbitrary units); *i*, *ii*, *iii*, and *iv* correspond to time points in the traces). The mean normalized trace for 10 cells is shown (*lower right panel*). The *red bar* indicates the time of hypotonic exposure. All images and analyses shown are a single representation contributing to the mean value quoted in the text and in Table 1.

remained at 20 ± 2% and 22 ± 5%, respectively, in control medium and increased to 75 ± 4% and 71 ± 7%, respectively, in hypotonic medium), indicating that an additional step is required in the translocation mechanism.

Hypotonic Stimulus Required for AQP1 Translocation Induces Increase in Intracellular Calcium—Following exposure to hypotonic conditions, the swelling response of many mammalian cells has been shown to be calcium-dependent (21, 22). To investigate a possible role for calcium in AQP1 translocation, we conducted real-time, intracellular calcium $[Ca^{2+}]_i$, imaging experiments using the fluorescent indicator Fluo-4 AM. Hypotonic stimulus (107–125 mosM/kg) induced a rapid $[Ca^{2+}]_i$ increase (40 ± 7% above basal levels; Fig. 3). We noted that the osmolality of the hypotonic stimulus that resulted in $[Ca^{2+}]_i$ elevations (Fig. 3) corresponded precisely with that required for wild-type AQP1 translocation and that both events occurred within the same timeframe (10–30 s) (19).

Extracellular Calcium Influx Is Necessary for Hypotonicity-induced AQP1 Translocation—To determine a role for hypotonicity-induced $[Ca^{2+}]_i$ elevations in the rapid regulation of AQP1 translocation, cells were incubated with 10 μM CPA for 30 min to inhibit intracellular calcium release from internal stores and then exposed to hypotonic conditions. An RME of 18 ± 4% in isotonic control medium and 71 ± 9% in hypotonic medium after 30 s indicated that depletion of intracellular calcium stores had little effect on AQP1 translocation (Fig. 4*A* and Table 1). In contrast, on removing extracellular calcium prior to hypotonic exposure, we observed only a transient translocation of AQP1-GFP in calcium-free medium followed by a return to basal RME levels (24 ± 4% within 120 s) despite continued incubation in hypotonic medium (Fig. 4*B* and Table 1). This is consistent with calcium release from intracellular stores being sufficient to induce transient translocation, but extracellular calcium entry being necessary for sustained membrane expression of AQP1. Indeed, similar results were obtained for cells in calcium-free medium in the presence of 10 μM CPA (RME was 23 ± 3% in control medium and 25 ± 5% in hypotonic medium; Fig. 4*C* and Table 1). For the mutant constructs, a $[Ca^{2+}]_i$, similar to that for wild-type AQP1-GFP, of 34 ± 5%, 32 ± 6%, 35 ± 4%, and 37 ± 6% above basal ($[Ca^{2+}]_i$) was measured for T157A, T239A, T157D, and T239D, respectively (Table 1). A $[Ca^{2+}]_i$ increase similar to that for wild-type AQP1-GFP was recorded for both double mutants (Table 1). In support of these observations, addition of caffeine alone, which has been shown to increase intracellular calcium concentration in HEK cells (26), did not stimulate sustained AQP1 membrane translocation in control medium (RME remained at 26 ± 4% in control medium and increased to 72 ± 6% in hypotonic medium). These results, together with the reversal of calcium elevation and AQP1 translocation upon cessation of hypotonic stimulus, illustrate the dynamic effects that fluctuating calcium levels have on AQP translocation.

Inhibition of Mechanosensitive TRP Channels Prevents Hypotonicity-induced AQP1 Translocation—Calcium-permeable TRP channels are involved in the response of mammalian cells to changes in extracellular osmolality (38). The stretch-activated TRP channel, TRPC1 (39, 40), is known to be present in HEK293 cells (41) and may be activated by the entry of water through the AQP1 channels that are already present in the membrane at a basal RME of 20 ± 3% (Table 1) (19). Table 1 shows that in the presence of the specific TRPC1 antagonist, SKF96365, hypotonicity-induced AQP1 translocation was ablated (RME was 26 ± 5% in control medium and 25 ± 6% in hypotonic medium).

Hypotonicity-induced AQP1 Translocation Is Mediated by Calmodulin—Incubation of cells expressing wild-type AQP1-GFP with 100 μM W7 calmodulin antagonist for 30 min inhibited hypotonicity-induced AQP1 translocation: RME values were 25 ± 4% in control medium and 28 ± 6% in hypotonic medium (Table 1). Furthermore, hypotonicity-induced subcellular localization of the T157D/T239D mutant was inhibited by preincubation of cells expressing this mutant with 100 μM W7 for 30 min (RME values for were 28 ± 5% in control medium and 22 ± 4% in hypotonic medium; Table 1). This suggested that, together with the requirement for specific PKC-dependent phosphorylation and calcium influx through TRP chan-

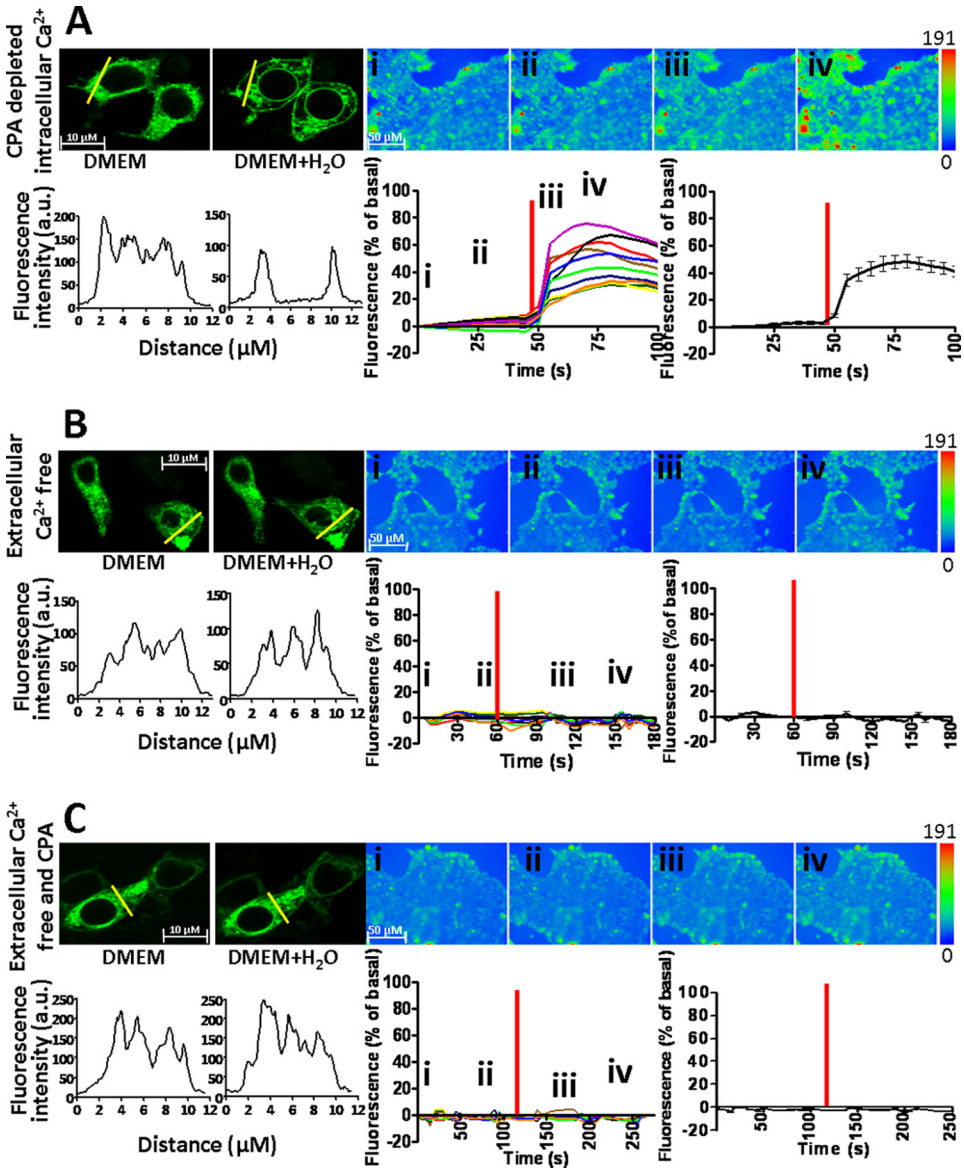

FIGURE 4. **Hypotonicity-induced intracellular Ca^{2+} elevations and AQP1 translocation in HEK293 cells cultured in calcium-free medium and/or with depleted intracellular calcium stores.** The subcellular localization of AQP1-GFP fusion proteins in HEK293 cells before and after hypotonic stimulus are shown (*A–C*; *left panels*), where the same cells are in control medium (*left panels*) and hypotonic medium (*right panels*). All measurements were taken at 48 h post-transfection. Fluorescence amplitudes along the line scans (in *yellow* on the image) are displayed graphically *below* each image, indicating subcellular localization of AQP1-GFP (*a.u.* is arbitrary units). *A* shows wild-type-like hypotonicity-induced AQP1-GFP translocation in the presence of 10 μM CPA. *B* shows no hypotonicity-induced AQP1-GFP translocation in Ca^{2+}-free medium. *C* shows no hypotonicity-induced AQP1-GFP translocation in Ca^{2+}-free medium with 10 μM CPA. The corresponding intracellular Ca^{2+} responses of the cells are shown (*upper right panels*) with mean normalized traces of fluorescence *versus* time shown below for 10 random cells from the images in the top panels (scale in arbitrary units); *i*, *ii*, *iii*, and *iv* correspond to time points in the traces. The mean normalized trace for 10 cells is shown to the *right*. The *red bar* indicates the time of hypotonic exposure. All images and analyses shown are a single representation contributing to the mean value quoted in the text and in Table 1.

nels, calmodulin is a further critical component of the AQP translocation mechanism.

DISCUSSION

There are 13 known members of the AQP family in humans (numbered AQP0 to AQP12), and they are found in different tissues throughout the body; wherever there is water (42). Impaired water homeostasis is associated with a wide range of conditions such as diabetes, high blood pressure, and brain swelling after stroke or head injury. These can become especially problematic as we age because the water content of our body declines from 60–65% of body mass in middle age to 50% by the age of 80 (43). Understanding the mechanisms of AQP regulation will therefore open up new avenues for therapeutic discovery.

Although recent advances have described AQP structure (5) and have established the mechanism of water selectivity through the AQP pore (3, 4), progress in understanding AQP regulation in mammalian cells has been limited to the role of AQP gene expression (9, 10) or AQP translocation via indirect G protein-coupled receptor networks (44) in the medium to long term (10). The latter has been comprehensively studied for AQP2: endocrine activation of vasopressin V_2 receptor is required for membrane localization of constitutive, intracellular AQP2 on a 15–60 min time scale (13, 14, 45). In this study,

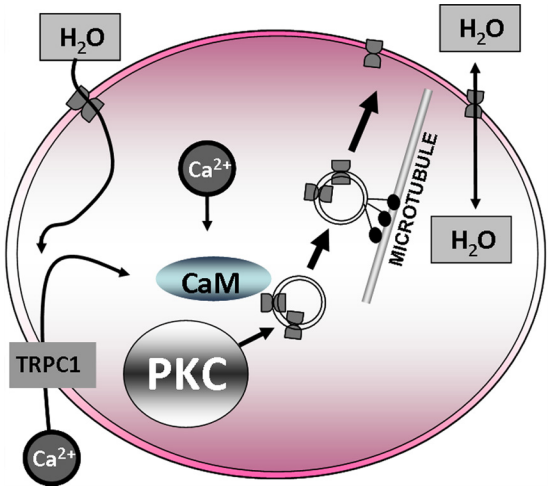

FIGURE 5. **A model for the direct regulation of rapid cellular water flow.** Influx of water by osmosis and/or through constitutively expressed AQP channels causes cell swelling and induces extracellular calcium entry through TRP channels, thereby triggering AQP1 translocation. This translocation along microtubules is dependent on calmodulin (*CaM*) activation and AQP1 phosphorylation by protein kinase C. Water subsequently enters or exits the cell to maintain cellular homeostasis.

we describe a physiologically relevant (Fig. 1) and direct mechanism for the regulation of functional AQP1 translocation (Fig. 2) on a timescale of seconds (Fig. 5). This mechanism incorporates our previous observation that AQP1 translocation is mediated by microtubules (19), which also have a role in AQP2 translocation (46).

Role for Calcium in Hypotonicity-induced AQP Translocation—The regulation of cell permeability via the action of AQP channels is central to the control of cell water transport and cell volume. Cells exposed to hypotonic stimuli often exhibit calcium elevations (47), although little is known about the role of this signal. The TRP calcium channel family can be activated by extracellular hypotonicity (48, 49), and members of this family have been shown to be involved in a hypotonicity-induced reduction of AQP5 abundance over a period of hours (50). However, to our knowledge, there is no previous indication that hypotonicity-induced calcium elevations directly induce a rapid translocation of AQPs. The findings in this study show that a cytosolic elevation of calcium following hypotonic stimulus evokes, and is necessary for, the translocation of AQP1 to the plasma membrane and that the inhibition of the TRP channel endogenous to HEK293 cells (TRPC1) prevents the hypotonicity-mediated subcellular localization of AQP1 to the plasma membrane. Furthermore, sustained translocation was induced in conditions where intracellular calcium stores were depleted, but only transient translocation, with no maintained plasma membrane localization, was induced in the absence of extracellular calcium, indicating that a calcium signal derived from extracellular or intracellular sources is sufficient. However, the absence of maintained plasma membrane localization with no external calcium, which would also lead to intracellular store depletion, shows that a sustained calcium signal is necessary for continued AQP1 plasma membrane localization. This is supported by the observations that a return to control medium and a reduction in calcium signal coincides with internalization of AQP1. Interestingly, as the sarco/endoplasmic reticulum Ca^{2+}-ATPase inhibitor, CPA, had no effect on sustained AQP1 localization, there may be no requirement for extracellular calcium to first pass through the intracellular stores. This may reflect that under normal conditions, the influx of extracellular calcium is the key requirement.

Phosphorylation-dependent Mechanism for Rapid, Direct Hypotonicity-induced AQP Translocation—The phosphorylation of AQPs is well established and several kinases are implicated in observed increases in water permeability, including protein kinases A and C, casein kinase II, and calcium/calmodulin kinase (9). We show that in addition to the requirement for calcium, hypotonicity-induced AQP1 translocation is both calmodulin- and PKC-dependent. The mechanism for the PKC-dependent nature of this movement requires the synergistic qualities of both known PKC phosphorylation sites of AQP1 (Thr-157 and Thr-239) (37). Neither residue, individually substituted with alanine or aspartate, caused any obvious phenotype under our experimental conditions. However a double alanine substitution (T157A/T239A) blocked all hypotonicity-mediated movement of AQP1. The fact that the T157D/T239D mutation did not result in constitutive plasma membrane localization is further consistent with our proposed mechanism in which hypotonicity-induced calcium elevations are sustained via extracellular-calcium influx and is mediated by calmodulin (Table 1): the calmodulin antagonist, W7, inhibited hypotonicity-induced AQP1 membrane localization but not hypotonicity-induced calcium elevations. It would appear that the T157D/T239D double mutation does not affect the calcium/calmodulin mechanism but rather mimics the charges induced by phosphorylation of Thr-157 and Thr-239, allowing translocation to occur. The calmodulin antagonist W7 inhibited hypotonicity-induced translocation of T157D/T239D but neither PKC inhibitor had any effect on hypotonicity-induced translocation of this construct. This T157D/T239D phosphomimetic AQP mutant is primed for translocation and therefore does not require PKC for membrane localization following hypotonicity-induced influx of extracellular calcium and activation of a calmodulin-dependent mechanism.

Implications—The speed of hypotonicity-induced AQP translocation suggests that constitutively expressed AQPs could participate in initial cell swelling. In many cells, this is often followed by a regulatory volume decrease, achieved by the efflux of ions by ion transporters and also organic osmolytes via volume-regulated anion channels. Our findings show that AQP1 translocation is also PKC- and calmodulin-dependent similar to the translocation of volume-regulated anion channels (51). It has also been suggested that hypotonicity may affect the translocation of sodium channels in cultured renal cell lines (52). Ion channel translocation in plant cells is known to be regulated by hydrostatic pressure (53, 54) and hypotonicity (55), whereas in animal cells, calcium-dependent exocytosis is a major mechanism for the release of neurotransmitters and hormones from neurones and endocrine cells (56).

In astrocytes, AQP1 is known to be involved in cell volume regulation and cerebral edema (57, 58). In the kidney, AQP1 knock-out mice suffer from polyuria (59, 60). AQP1 (unlike AQP2 in the collecting duct) is extensively found in the renal proximal tubule and thin descending limb of Henle, the two

regions responsible for reabsorbing 80% of the fluid from the glomerular filtrate (61). It may be that the quickest response of AQP1-expressing astrocytes and kidney cells to an increase in cellular water levels is a hypotonicity-mediated increase in available AQP1 at the appropriate membrane surface, as suggested by studies of the long term expression of AQP1 (62). The mechanisms underpinning AQP1 regulation therefore have the potential to be manipulated for therapeutic benefit.

In conclusion, we have shown that rapid AQP1 translocation involves calcium signaling indicating that this mechanism mediates control of cellular water permeability in response to physiological stimuli. As hypotonicity-induced translocation of AQP1 involves ubiquitous and pluripotent calcium, the data described here may serve as a universal prototype for rapid and direct regulation of this important protein family.

REFERENCES

1. Benga, G., Popescu, O., Borza, V., Pop, V. I., Muresan, A., Mocsy, I., Brain, A., and Wrigglesworth, J. M. (1986) Water permeability in human erythrocytes: Identification of membrane proteins involved in water transport. *Eur. J. Cell Biol.* **41,** 252–262
2. Nielsen, S., Smith, B. L., Christensen, E. I., and Agre, P. (1993) Distribution of the aquaporin CHIP in secretory and resorptive epithelia and capillary endothelia. *Proc. Natl. Acad. Sci. U.S.A.* **90,** 7275–7279
3. de Groot, B. L., Frigato, T., Helms, V., and Grubmüller, H. (2003) The mechanism of proton exclusion in the aquaporin-1 water channel. *J. Mol. Biol.* **333,** 279–293
4. de Groot, B. L., and Grubmüller, H. (2001) Water permeation across biological membranes: Mechanism and dynamics of aquaporin-1 and GlpF. *Science* **294,** 2353–2357
5. Walz, T., Fujiyoshi, Y., and Engel, A. (2009) The AQP structure and functional implications. *Handb. Exp. Pharmacol.* **190,** 31–56
6. Litman, T., Søgaard, R., and Zeuthen, T. (2009) Ammonia and urea permeability of mammalian aquaporins. *Handb. Exp. Pharmacol.* **190,** 327–358
7. Törnroth-Horsefield, S., Wang, Y., Hedfalk, K., Johanson, U., Karlsson, M., Tajkhorshid, E., Neutze, R., and Kjellbom, P. (2006) Structural mechanism of plant aquaporin gating. *Nature* **439,** 688–694
8. Wang, Y., and Tajkhorshid, E. (2007) Molecular mechanisms of conduction and selectivity in aquaporin water channels. *J. Nutr.* **137,** 1509S–1515S
9. Gunnarson, E., Zelenina, M., and Aperia, A. (2004) Regulation of brain aquaporins. *Neuroscience* **129,** 947–955
10. Zelenina, M. (2010) Regulation of brain aquaporins. *Neurochem. Int.* **57,** 468–488
11. Hoffmann, E. K., Lambert, I. H., and Pedersen, S. F. (2009) Physiology of cell volume regulation in vertebrates. *Physiol. Rev.* **89,** 193–277
12. Pasantes-Morales, H., and Cruz-Rangel, S. (2010) Brain volume regulation: Osmolytes and aquaporin perspectives. *Neuroscience* **168,** 871–884
13. Fenton, R. A., Moeller, H. B., Hoffert, J. D., Yu, M. J., Nielsen, S., and Knepper, M. A. (2008) Acute regulation of aquaporin-2 phosphorylation at Ser-264 by vasopressin. *Proc. Natl. Acad. Sci. U.S.A.* **105,** 3134–3139
14. Hoffert, J. D., Nielsen, J., Yu, M. J., Pisitkun, T., Schleicher, S. M., Nielsen, S., and Knepper, M. A. (2007) Dynamics of aquaporin-2 serine-261 phosphorylation in response to short term vasopressin treatment in collecting duct. *Am. J. Physiol. Renal Physiol.* **292,** F691–700
15. Noda, Y., and Sasaki, S. (2005) Trafficking mechanism of water channel aquaporin-2. *Biol. Cell* **97,** 885–892
16. Marinelli, R. A., Pham, L., Agre, P., and LaRusso, N. F. (1997) Secretin promotes osmotic water transport in rat cholangiocytes by increasing aquaporin-1 water channels in plasma membrane. Evidence for a secretin-induced vesicular translocation of aquaporin-1. *J. Biol. Chem.* **272,** 12984–12988
17. Yasui, H., Kubota, M., Iguchi, K., Usui, S., Kiho, T., and Hirano, K. (2008) Membrane trafficking of aquaporin 3 induced by epinephrine. *Biochem. Biophys. Res. Commun.* **373,** 613–617
18. Ishikawa, Y., Iida, H., and Ishida, H. (2002) The muscarinic acetylcholine receptor-stimulated increase in aquaporin-5 levels in the apical plasma membrane in rat parotid acinar cells is coupled with activation of nitric oxide/cGMP signal transduction. *Mol. Pharmacol.* **61,** 1423–1434
19. Conner, M. T., Conner, A. C., Brown, J. E., and Bill, R. M. (2010) Membrane trafficking of aquaporin 1 is mediated by protein kinase C via microtubules and regulated by tonicity. *Biochemistry* **49,** 821–823
20. Benfenati, V., and Ferroni, S. (2010) Water transport between CNS compartments: Functional and molecular interactions between aquaporins and ion channels. *Neuroscience* **168,** 926–940
21. Eveloff, J. L., and Warnock, D. G. (1987) Activation of ion transport systems during cell volume regulation. *Am. J. Physiol.* **252,** F1–10
22. Benfenati, V., Caprini, M., Dovizio, M., Mylonakou, M. N., Ferroni, S., Ottersen, O. P., and Amiry-Moghaddam, M. (2011) An aquaporin-4-transient receptor potential vanilloid 4 (AQP4-TRPV4) complex is essential for cell-volume control in astrocytes. *Proc. Natl. Acad. Sci. U.S.A.* **108,** 2563–2568
23. Acs, P., Bögi, K., Lorenzo, P. S., Marquez, A. M., Bíró, T., Szállási, Z., and Blumberg, P. M. (1997) The catalytic domain of protein kinase C chimeras modulates the affinity and targeting of phorbol ester-induced translocation. *J. Biol. Chem.* **272,** 22148–22153
24. Nishizuka, Y. (1986) Studies and perspectives of protein kinase C. *Science* **233,** 305–312
25. Rane, S. G., and Dunlap, K. (1986) Kinase C activator 1,2-oleoylacetylglycerol attenuates voltage-dependent calcium current in sensory neurons. *Proc. Natl. Acad. Sci. U.S.A.* **83,** 184–188
26. Querfurth, H. W., Haughey, N. J., Greenway, S. C., Yacono, P. W., Golan, D. E., and Geiger, J. D. (1998) Expression of ryanodine receptors in human embryonic kidney (HEK293) cells. *Biochem. J.* **334,** 79–86
27. Hidaka, H., Yamaki, T., Naka, M., Tanaka, T., Hayashi, H., and Kobayashi, R. (1980) Calcium-regulated modulator protein interacting agents inhibit smooth muscle calcium-stimulated protein kinase and ATPase. *Mol. Pharmacol.* **17,** 66–72
28. Nesic, O., Lee, J., Unabia, G. C., Johnson, K., Ye, Z., Vergara, L., Hulsebosch, C. E., and Perez-Polo, J. R. (2008) Aquaporin 1, a novel player in spinal cord injury. *J. Neurochem.* **105,** 628–640
29. Singh, A., Hildebrand, M. E., Garcia, E., and Snutch, T. P. (2010) The transient receptor potential channel antagonist SKF96365 is a potent blocker of low voltage-activated T-type calcium channels. *Br. J. Pharmacol.* **160,** 1464–1475
30. Kocanova, S., Hornakova, T., Hritz, J., Jancura, D., Chorvat, D., Mateasik, A., Ulicny, J., Refregiers, M., Maurizot, J. C., and Miskovsky, P. (2006) Characterization of the interaction of hypericin with protein kinase C in U-87 MG human glioma cells. *Photochem. Photobiol.* **82,** 720–728
31. Laursen, M., Bublitz, M., Moncoq, K., Olesen, C., Møller, J. V., Young, H. S., Nissen, P., and Morth, J. P. (2009) Cyclopiazonic acid is complexed to a divalent metal ion when bound to the sarcoplasmic reticulum Ca^{2+}-ATPase. *J. Biol. Chem.* **284,** 13513–13518
32. Conner, M., Hawtin, S. R., Simms, J., Wootten, D., Lawson, Z., Conner, A. C., Parslow, R. A., and Wheatley, M. (2007) Systematic analysis of the entire second extracellular loop of the V(1a) vasopressin receptor: Key residues, conserved throughout a G protein-coupled receptor family, identified. *J. Biol. Chem.* **282,** 17405–17412
33. Parri, H. R., Gould, T. M., and Crunelli, V. (2010) Sensory and cortical activation of distinct glial cell subtypes in the somatosensory thalamus of young rats. *Eur. J. Neurosci.* **32,** 29–40
34. Maric, K., Wiesner, B., Lorenz, D., Klussmann, E., Betz, T., and Rosenthal, W. (2001) Cell volume kinetics of adherent epithelial cells measured by laser scanning reflection microscopy: Determination of water permeability changes of renal principal cells. *Biophys. J.* **80,** 1783–1790
35. Krane, C. M., and Goldstein, D. L. (2007) Comparative functional analysis of aquaporins/glyceroporins in mammals and anurans. *Mamm. Genome* **18,** 452–462
36. Satoh, J., Tabunoki, H., Yamamura, T., Arima, K., and Konno, H. (2007) Human astrocytes express aquaporin-1 and aquaporin-4 *in vitro* and *in vivo*. *Neuropathology* **27,** 245–256
37. Zhang, W., Zitron, E., Hömme, M., Kihm, L., Morath, C., Scherer, D.,

Hegge, S., Thomas, D., Schmitt, C. P., Zeier, M., Katus, H., Karle, C., and Schwenger, V. (2007) Aquaporin-1 channel function is positively regulated by protein kinase C. *J. Biol. Chem.* **282,** 20933–20940
38. Vriens, J., Watanabe, H., Janssens, A., Droogmans, G., Voets, T., and Nilius, B. (2004) Cell swelling, heat, and chemical agonists use distinct pathways for the activation of the cation channel TRPV4. *Proc. Natl. Acad. Sci. U.S.A.* **101,** 396–401
39. Beech, D. J. (2005) TRPC1: Store-operated channel and more. *Pflugers Arch.* **451,** 53–60
40. Maroto, R., Raso, A., Wood, T. G., Kurosky, A., Martinac, B., and Hamill, O. P. (2005) TRPC1 forms the stretch-activated cation channel in vertebrate cells. *Nat. Cell Biol.* **7,** 179–185
41. Beech, D. J., Xu, S. Z., McHugh, D., and Flemming, R. (2003) TRPC1 store-operated cationic channel subunit. *Cell Calcium.* **33,** 433–440
42. Agre, P. (2006) The aquaporin water channels. *Proc. Am. Thorac. Soc.* **3,** 5–13
43. Luckey, A. E., and Parsa, C. J. (2003) Fluid and electrolytes in the aged. *Arch. Surg.* **138,** 1055–1060
44. Nedvetsky, P. I., Tamma, G., Beulshausen, S., Valenti, G., Rosenthal, W., and Klussmann, E. (2009) Regulation of aquaporin-2 trafficking. *Handb. Exp. Pharmacol.* **190,** 133–157
45. Fenton, R. A., and Moeller, H. B. (2008) Recent discoveries in vasopressin-regulated aquaporin-2 trafficking. *Prog. Brain Res.* **170,** 571–579
46. Brown, D., Katsura, T., and Gustafson, C. E. (1998) Cellular mechanisms of aquaporin trafficking. *Am. J. Physiol.* **275,** F328–331
47. Ding, Y., Schwartz, D., Posner, P., and Zhong, J. (2004) Hypotonic swelling stimulates L-type Ca^{2+} channel activity in vascular smooth muscle cells through PKC. *Am. J. Physiol. Cell Physiol.* **287,** C413–421
48. Liedtke, W., Choe, Y., Martí-Renom, M. A., Bell, A. M., Denis, C. S., Sali, A., Hudspeth, A. J., Friedman, J. M., and Heller, S. (2000) Vanilloid receptor-related osmotically activated channel (VR-OAC), a candidate vertebrate osmoreceptor. *Cell* **103,** 525–535
49. Nilius, B., Vriens, J., Prenen, J., Droogmans, G., and Voets, T. (2004) TRPV4 calcium entry channel: A paradigm for gating diversity. *Am. J. Physiol. Cell Physiol.* **286,** C195–205
50. Sidhaye, V. K., Güler, A. D., Schweitzer, K. S., D'Alessio, F., Caterina, M. J., and King, L. S. (2006) Transient receptor potential vanilloid 4 regulates aquaporin-5 abundance under hypotonic conditions. *Proc. Natl. Acad. Sci. U.S.A.* **103,** 4747–4752
51. Fisher, S. K., Cheema, T. A., Foster, D. J., and Heacock, A. M. (2008) Volume-dependent osmolyte efflux from neural tissues: regulation by G protein-coupled receptors. *J. Neurochem.* **106,** 1998–2014
52. Jans, D., Simaels, J., Cucu, D., Zeiske, W., and Van Driessche, W. (2000) Effects of extracellular Mg^{2+} on transepithelial capacitance and Na^+ transport in A6 cells under different osmotic conditions. *Pflugers Arch.* **439,** 504–512
53. Homann, U., and Thiel, G. (2002) The number of K^+ channels in the plasma membrane of guard cell protoplasts changes in parallel with the surface area. *Proc. Natl. Acad. Sci. U.S.A.* **99,** 10215–10220
54. Zorec, R., and Tester, M. (1993) Rapid pressure-driven exocytosis-endocytosis cycle in a single plant cell. Capacitance measurements in aleurone protoplasts. *FEBS Lett.* **333,** 283–286
55. Liu, K., and Luan, S. (1998) Voltage-dependent K^+ channels as targets of osmosensing in guard cells. *Plant Cell* **10,** 1957–1970
56. Dolenšek, J., Skelin, M., and Rupnik, M. S. (2011) Calcium dependencies of regulated exocytosis in different endocrine cells. *Physiol. Res.* **60,** S29–38
57. McCoy, E., and Sontheimer, H. (2010) MAPK induces AQP1 expression in astrocytes following injury. *Glia* **58,** 209–217
58. McCoy, E. S., Haas, B. R., and Sontheimer, H. (2010) Water permeability through aquaporin-4 is regulated by protein kinase C and becomes rate-limiting for glioma invasion. *Neuroscience* **168,** 971–981
59. Schnermann, J., Chou, C. L., Ma, T., Traynor, T., Knepper, M. A., and Verkman, A. S. (1998) Defective proximal tubular fluid reabsorption in transgenic aquaporin-1 null mice. *Proc. Natl. Acad. Sci. U.S.A.* **95,** 9660–9664
60. Yang, B., Ma, T., Dong, J. Y., and Verkman, A. S. (2000) Partial correction of the urinary concentrating defect in aquaporin-1 null mice by adenovirus-mediated gene delivery. *Hum. Gene Ther.* **11,** 567–575
61. Lankford, S. P., Chou, C. L., Terada, Y., Wall, S. M., Wade, J. B., and Knepper, M. A. (1991) Regulation of collecting duct water permeability independent of cAMP-mediated AVP response. *Am. J. Physiol.* **261,** F554–566
62. Bouley, R., Palomino, Z., Tang, S. S., Nunes, P., Kobori, H., Lu, H. A., Shum, W. W., Sabolic, I., Brown, D., Ingelfinger, J. R., and Jung, F. F. (2009) Angiotensin II and hypertonicity modulate proximal tubular aquaporin 1 expression. *Am. J. Physiol. Renal Physiol.* **297,** F1575–1586